Special Issue Article

Institution of MECHANICAL ENGINEERS
Journal of SYSTEMS AND CONTROL ENGINEERING

Proc IMechE Part I:
J Systems and Control Engineering
2019, Vol. 233(7) 788–800

DOI: 10.1177/0959651818823589
journals.sagepub.com/home/pii
SAGE

Torque vectoring–based drive: Assistance system for turning an electric narrow tilting vehicle

Yaxing Ren[1], Truong Quang Dinh[2], James Marco[2] and David Greenwood[2]

Abstract

The increasing number of cars leads to traffic congestion and limits parking issue in urban area. The narrow tilting vehicles therefore can potentially become the next generation of city cars due to its narrow width. However, due to the difficulty in leaning a narrow tilting vehicle, a drive assistance strategy is required to maintain its roll stability during a turn. This article presents an effective approach using torque vectoring method to assist the rider in balancing the narrow tilting vehicles, thus reducing the counter-steering requirements. The proposed approach is designed as the combination of two torque controllers: steer angle–based torque vectoring controller and tilting compensator–based torque vectoring controller. The steer angle–based torque vectoring controller reduces the counter-steering process via adjusting the vectoring torque based on the steering angle from the rider. Meanwhile, the tilting compensator–based torque vectoring controller develops the steer angle–based torque vectoring with an additional tilting compensator to help balancing the leaning behaviour of narrow tilting vehicles. Numerical simulations with a number of case studies have been carried out to verify the performance of designed controllers. The results imply that the counter-steering process can be eliminated and the roll stability performance can be improved with the usage of the presented approach.

Keywords

Roll stability, torque vectoring, drive assistance, narrow tilting vehicle

Date received: 3 July 2018; accepted: 2 December 2018

Introduction

Considering the practical dimensions and low energy consumption, electric vehicles are expected to be the main transportation in a near future. The increasing number of cars leads to traffic congestion and limits parking places in urban area. Due to this issue, small narrow commuter vehicles are required to become a new generation of city cars,[1] as the two prototype vehicles developed in the Range of Electric SOlutions for L-category VEhicles (RESOLVE) project shown in Figure 1. The narrow commuter vehicles have four wheels like a car but with just half the width of a conventional car, like a motorcycle. This makes a narrow commuter vehicle integrate the features and advantages of a car and a motorcycle, but its roll stability is an issue.[3–6]

In order to maintain lateral stability, the narrow commuter vehicles should lean into corners during turning like two-wheeled vehicles.[7,8] This type of vehicle is also called a narrow tilting vehicle (NTV). Different from the conventional vehicles that have roll stiffness to balance the roll stability by its own suspension structure, the NTV has no such roll stiffness. Thus, the NTVs fall down easily during a turn if its roll stability cannot be well maintained. This is the main challenge in NTVs.

Unlike the case of a motorcycle, in which the rider can shift his weight to lean the motorcycle into a corner, the mass of an NTV is much higher than that of a human body.[7] The rider has to act on the counter-steering and throttle to balance the vehicle in a turn.[7,8] In normal steering method, a rider has to manage the following actions:

[1]School of Engineering, University of Glasgow, Glasgow, UK
[2]Warwick Manufacturing Group (WMG), University of Warwick, Coventry, UK

Corresponding author:
James Marco, Warwick Manufacturing Group (WMG), University of Warwick, Coventry, CV4 7AL, UK.
Email: James.Marco@warwick.ac.uk

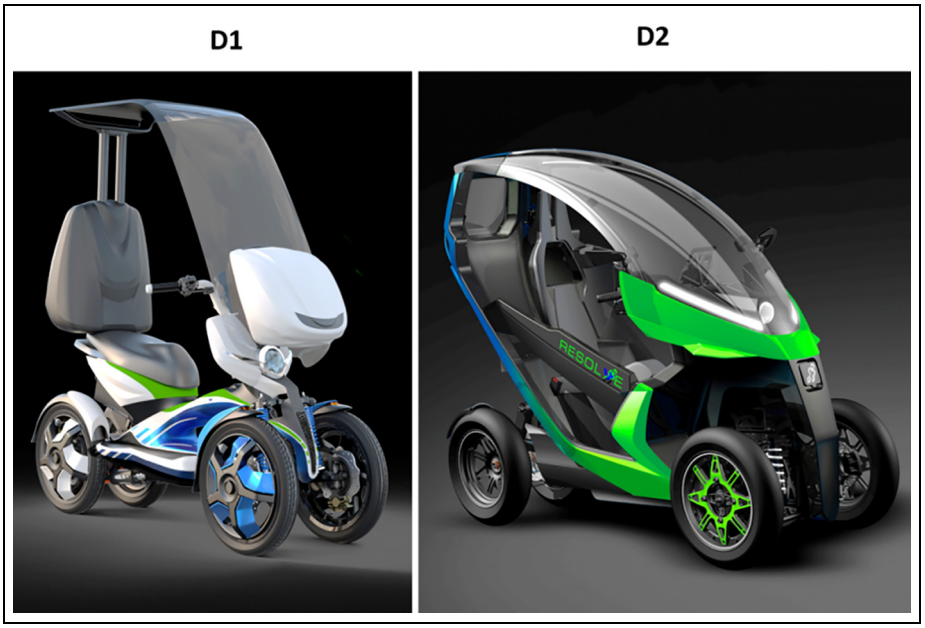

Figure 1. Two demonstrators of narrow tilting vehicle developed in the RESOLVE project.[2]

1. Provide a counter-steering on the throttle;
2. Provide the lateral force causing a yaw rate to the opposite direction and a roll rate to the desired direction;
3. Turn the steering to the desired direction shortly after the counter-steering;
4. Create the vehicle yawing to the desired direction.

The riders of NTVs are required to be very experienced in controlling the vehicle in balancing and path following. However, the next-generation vehicle should be much easier to be ridden by any type of riders, from new to experienced. Therefore, it is required to develop an assistance system for the rider in tilting and balancing the NTV.

From literature, the common solution to solve this issue is to use external mechanisms for the active tilting control. The two main tilting methods are the steering tilt control (STC) and the direct tilt control (DTC),[9,10] one aims to control directly on the steering angle and the other aims to provide additional moment of torque to tilt the vehicle. As studied in previous research works, the STC system is efficient at high speed but the balancing does not suit well at the standstill or at very low speed and performs even worse in slippery road conditions.[11] The DTC system simplifies the control with an additional tilt actuator but it requires high tilting motion and the delayed actuator response causes the risk of vehicle oscillations.[12] Both the approaches require additional mechanisms to adjust the performance of the vehicle following rider's behaviour. This article presents an alternative way of using torque vectoring (TV) techniques to assist the rider in balancing the NTV and simplify the steering process of turning the NTV without any additional mechanisms, as shown in Figure 2.

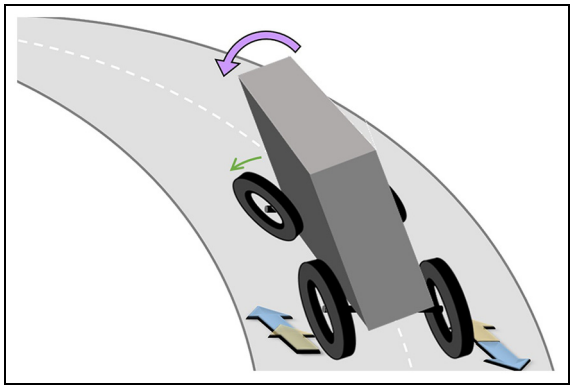

Figure 2. Torque vectoring assists the rider in balancing the NTV during a turn.

The traditional TV technology can improve the vehicle cornering response and it has the potential to improve the handling response of a vehicle.[13] The first left–right TV technique proposed by Sawase and Sano[14] aims to distributing driving and braking forces acting upon the right and left wheels in a wheel-individual vehicle.[15] The different mechanisms and control allocation criteria have been reviewed and compared for their performances and sensitivities to electric motor drive parameters in the works by De Novellis et al.[13] and Sawase and colleagues.[16,17] The maximum vectoring torque limit has been determined by Sawase and Ushiroda[17] and desired traction force and yaw moment input has been mapped by Kang et al.[18] using an optimal TV algorithm. In recent literature, the TV approach has been optimized to improve the yaw moment distraction performance,[19] improve its stability under expected road and driving conditions,[20]

maximize the driving velocity and enhance the lateral stability in cornering,[21] and minimize the power losses on a battery electric vehicle.[15] In these approaches, the TV method is used as assistant torque for vehicle yaw turn in normal vehicles as its roll stability is not a main issue. However, more attention needs to be paid in the roll stability maintenance in an NTV and the conventional TV method is not suitable to be used in this type of vehicles. In this point of view, none of the previously designed torque controllers has considered the feature of NTV to assist the rider in balancing the vehicle in a turn using TV technology.

This article aims to develop and implement the TV technology to assist the rider to maintain the roll dynamics of NTV in corners. The proposed approach is designed as the combination of two torque controllers: steer angle–based torque vectoring (SATV) controller and tilting compensator–based torque vectoring (TCTV) controller. The SATV controller manages the vectoring torque based on the steer angle in order to reduce the counter-steering process, while the TCTV controller uses a further tilting compensator to improve the tilting stability of NTVs. The developed TV controllers have the ability to reduce the counter-steering requirements from the rider and improve the tilting behaviour during turning an NTV. As a result, both the new rider and experienced rider can drive the NTV easily.

Mathematical model of four-wheel vehicle dynamics

Wheel dynamics

In the rear-wheel-drive vehicles, the wheel speed ω_{ij} is presented to describe the power transfer from wheel hub to road as follows[5,22]

$$\dot{\omega}_{fj} = -T_{brk,f} - R_f F_{l,fj} J_{fj} \tag{1}$$

$$\dot{\omega}_{rj} = T_{rj} - T_{brk,r} - R_r F_{l,rj} J_{rj} \tag{2}$$

where J_{ij} is the wheels' inertia around the wheel with the radius R_i with $ij \in \{fl, fr, rl, rr\}$ that represent the front left, front right, rear left, and rear right wheels, respectively. The wheels are driven by the torque T_{rj} that is applied on the left and right rear wheels that are resistant by the brake torque $T_{brk,i}$ and longitudinal force $F_{l,ij}$ at the contact point between road and tyre. The longitudinal force can be described as a function of friction coefficient μ_{ij} and tyre longitudinal slip $s_{l,ij}$

$$F_{l,ij} = F_{z,ij} \cdot \mu_{ij}(s_{l,ij}) \tag{3}$$

The tyre characteristics are modelled by the *magic tyre formula* in the research by Pacejka[23] as follows

$$\mu_{ij}(x_{ij}) = \sin\{C \arctan[B(1-E) \cdot x_{ij} + E \arctan(B \cdot x_{ij})]\} \tag{4}$$

where B, C, and E are tyre parameters determined by measurements; x_{ij} can be the longitudinal slip $s_{l,ij}$ or lateral slip angle α_{ij} to calculate the longitudinal slip force or side-slip force.[24] $F_{z,ij}$ is the vertical load of each wheel that can be calculated as follows

$$F_{z,fl} = m\left(\frac{l_r}{l}g - \frac{h}{l}a_x\right)\left(\frac{1}{2} - \frac{h}{b_f}\frac{a_y}{g}\right) \tag{5}$$

$$F_{z,fr} = m\left(\frac{l_r}{l}g - \frac{h}{l}a_x\right)\left(\frac{1}{2} + \frac{h}{b_f}\frac{a_y}{g}\right) \tag{6}$$

$$F_{z,rl} = m\left(\frac{l_f}{l}g + \frac{h}{l}a_x\right)\left(\frac{1}{2} - \frac{h}{b_r}\frac{a_y}{g}\right) \tag{7}$$

$$F_{z,rr} = m\left(\frac{l_f}{l}g + \frac{h}{l}a_x\right)\left(\frac{1}{2} + \frac{h}{b_r}\frac{a_y}{g}\right) \tag{8}$$

where m is the vehicle mass, l is the wheelbase which consists of the distance from the centre of gravity (COG) to the front and rear axles as l_f and l_r, h is the height of vehicle COG from the road surface, b_f and b_r are the track of front and rear axles, and g is the gravitational constant. a_x and a_y are the vehicle acceleration in x- and y-axes.

And tyre longitudinal slip $s_{l,ij}$ can be described based on the vehicle velocity v and vehicle side-slip angle β as follows

$$s_{l,ij} = R_i\omega_{ij} - v\cos\beta \max(R_i\omega_{ij}, v\cos\beta) \tag{9}$$

The side-slip force of tyre is also represented by the magic tyre formula in equation (4) as follows

$$F_{s,ij} = F_{z,ij} \cdot [\mu_{ij}(\alpha_{ij}) + \lambda_{st}\theta] \tag{10}$$

where λ_{st} is the camber stiffness coefficient of tyre and θ is the roll angle of tilting vehicle. The lateral slip angle of front and rear wheels α_{ij} is the angle between the wheels' velocity vector and its longitudinal axis, which can be can be calculated as follows

$$\alpha_{fj} = \delta - \arctan\left(\frac{v\sin\beta + l_f\dot{\varphi}}{v\cos\beta}\right) \tag{11}$$

$$\alpha_{rj} = -\arctan\left(\frac{v\sin\beta - l_r\dot{\varphi}}{v\cos\beta}\right) \tag{12}$$

where δ is the steering angle of front wheels, and $\dot{\varphi}$ is the yaw rate of the vehicle.

To present the forces in the vehicle-fixed coordinate system, the traction force of front wheels $F_{x,fj}$ and lateral force of front wheels $F_{y,fj}$ are given by the transformation

$$F_{x,fj} = F_{l,fj}\cos\delta - F_{s,fj}\sin\delta \tag{13}$$

$$F_{y,fj} = F_{l,fj}\sin\delta + F_{s,fj}\cos\delta \tag{14}$$

and the traction and lateral forces of rear wheels $F_{x,rj}$ and $F_{y,rj}$ are calculated equal to the longitudinal and side-slip forces $F_{l,rj}$ and $F_{s,rj}$, respectively.

Vehicle dynamics

The vehicle model of NTV includes velocity dynamic, side-slip angle dynamic, yaw dynamic, and roll dynamic.[15] The geometry model of an NTV is shown in Figure 3. The vehicle motion dynamics can be described by the vehicle velocity v and the vehicle side-slip angle β, which is defined as the angle between v and the vehicle longitudinal axis x. Their dynamics can be represented by the following differential equations

$$\dot{v} = \frac{1}{m}\left(\cos\beta \sum_{ij} F_{x,ij} + \sin\beta \sum_{ij} F_{y,ij} - F_{res}\right) \quad (15)$$

$$\dot{\beta} = \frac{1}{mv}\left(\cos\beta \sum_{ij} F_{y,ij} - \sin\beta \sum_{ij} F_{x,ij}\right) - \dot{\varphi} \quad (16)$$

where F_{res} represents the force of driving resistance.

The vehicle acceleration can be calculated by the relationship of v, β, ϕ, and their differentials as follows

$$a_x = \dot{v}\cos\beta - v\left(\dot{\beta} + \dot{\varphi}\right)\sin\beta \quad (17)$$

$$a_y = \dot{v}\sin\beta + v\left(\dot{\beta} + \dot{\varphi}\right)\cos\beta \quad (18)$$

The yaw motion of the vehicle can be calculated as the differential equation

$$\ddot{\varphi} = \frac{1}{I_z}\left[l_f\left(F_{y,fl} + F_{y,fr}\right) - l_r\left(F_{y,rl} + F_{y,rr}\right) + \frac{b_f}{2}\left(F_{x,fr} - F_{x,fl}\right) + \frac{b_r}{2}\left(F_{x,rr} - F_{x,rl}\right)\right] \quad (19)$$

where I_z is the inertia moment about the vertical axis.

Different from the roll damping dynamic of normal vehicles, the NTV has no roll stiffness of suspension. Thus, it is not self-stable in the roll motion and could finally fall down. The equation of roll motion of NTV is described as follows

$$\ddot{\theta} = 1I_x + mh^2\sin^2\theta\left[mhg\sin\theta - h\cos\theta\sum F_{y,ij} - mh^2\dot{\theta}^2\sin\theta\cos\theta - C_d\dot{\theta}\right] \quad (20)$$

where θ and $\dot{\theta}$ are the vehicle roll angle and roll rate, I_x is the vehicle roll moment of inertia, and C_d is the roll damping ratio of the suspension.

TV control system design

Simplified single-track vehicle model

The nonlinear equations of the four-wheel model provided in the previous section are much more accurate in matching the real vehicle response. However, the complex nonlinear equations and the interactions between states are difficult to be used in controller design and performance analysis. Therefore, a simplified single-track model has been delivered from the nonlinear equations (1)–(20). To simplify the model, it is assumed that the steer angle, side-slip angle, and roll angle are small and equal to their sinusoidal value; the COG is at the middle of the vehicle track ($l_f = l_r$); and the rear wheel torque differential value ΔT_r is defined as an additional system input. Then, the vehicle model can be represented as a function of the system space vector x and control vector u as follows

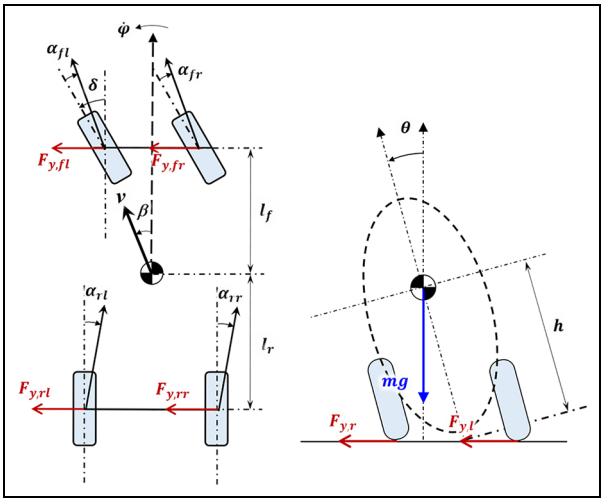

Figure 3. Geometry model of a narrow tilting vehicle.

$$\dot{x} = f(x) + g(x)\cdot u \quad (21)$$

where

$$x = \begin{bmatrix} v & \beta & \dot{\varphi} & \theta & \dot{\theta} \end{bmatrix}^T,\ u = \begin{bmatrix} \delta & T_r & \Delta T_r \end{bmatrix}^T \quad (22)$$

$$f(x) = \begin{bmatrix} -\frac{2C_\gamma}{m}\beta^2 + \frac{2\lambda_\gamma}{m}\beta\theta \\ -\frac{2C_\gamma}{m}\frac{\beta}{v} + \frac{2\lambda_\gamma}{m}\frac{\theta}{v} - \dot{\varphi} \\ -\frac{C_\gamma l^2}{2I_z}\frac{\dot{\varphi}}{v} \\ \dot{\theta} \\ \frac{mgh-2\lambda_\gamma h}{I_x}\theta - \frac{C_d}{I_x}\dot{\theta} + \frac{2C_\gamma h}{I_x}\beta - \frac{mh^2}{I_x}\dot{\theta}^2\theta \end{bmatrix} \quad (23)$$

$$g(x) = \begin{bmatrix} \frac{C_\gamma}{m}\beta & \frac{1}{mR_r} & 0 \\ \frac{C_\gamma}{mv} & -\frac{\beta}{mv} & 0 \\ \frac{C_\gamma l}{2I_z}\beta & 0 & \frac{b_r}{I_z} \\ 0 & 0 & 0 \\ -\frac{C_\gamma h}{I_x} & 0 & 0 \end{bmatrix} \quad (24)$$

including the linearized tyre lateral behaviour as equivalent cornering stiffness coefficient C_γ and camber stiffness coefficient λ_γ.

The system will finally converge to its steady state with a given trajectory by assuming that the deviations of system states are all zero. When the vehicle is turning in a circle with radius of R, the system steady-state value of side-slip angle, yaw rate, and roll angle can be approximately calculated as follows

$$\begin{cases} \beta_0 = l/2R \\ \dot{\varphi}_0 = v/R \\ \theta_0 = v^2/gR \end{cases} \tag{25}$$

Virtual rider model

Steering control. This rider robot had two control aims: to maintain standing stability and to follow a target course.[7] In turning an NTV, the rider has to act on the counter-steering and throttle to balance the NTV in a turn. The NTV stability control algorithm needs to be developed considering as the rider has no special operating skills.[12,25,26] One solution is to apply two separate control algorithms, one to maintain the roll angle and the other to follow the path, and then put together the two systems to form the control algorithm for NTV.

In rider's roll stability control, a proportional derivative (PD) control algorithm was applied to maintain the roll angle[7] as follows

$$\delta_1 = \left(k_{p2} + sk_{d2}\right)\left(\theta_{ref} - \theta\right) \tag{26}$$

In rider's lateral control, the rider implements on steering input to follow a certain desired lateral trajectory without regard to vehicle tilt stability, where the relationship between the path and steering angle is assumed to be linear.[7] The transient response of the lateral trajectory tracking is not urgent comparing with the roll stability control. Due to this, a pseudo-derivative feedback (PDF) control algorithm is applied to reduce the effect of derivative feed-forward action comparing with a traditional PI(D) control.[27] The lateral control of the virtual rider that presents the steering angle for lateral trajectory tracking can then be designed as follows

$$\delta_2 = \frac{k_{i1}}{s}\left(\dot{\varphi}_{ref} - \dot{\varphi}\right) - k_{p1}\dot{\varphi} \tag{27}$$

Then, the two systems will be combined together in the virtual rider model

$$\delta = \delta_1 + \delta_2 \tag{28}$$

Speed control. Apart from the steering control to follow the path and maintain the roll stability, the rider also has to control the vehicle speed via throttle. The sensor installed in throttle sends the position information to the controller to indicate the rider's torque demand. Then, a torque reference is sent to the inverter control unit to drive the wheel motors. To simplify this process, the speed control is presented via a PI controller as the rider aims to track the target vehicle velocity

$$T_r = \left(k_{p3} + \frac{k_{i3}}{s}\right)\left(V_{ref} - v\right) \tag{29}$$

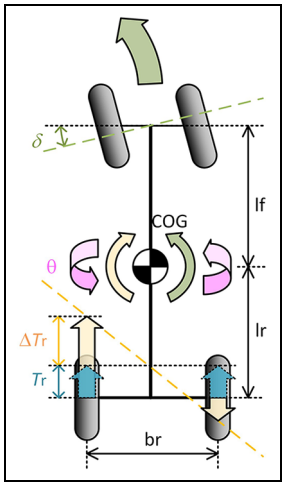

Figure 4. The diagram of torque vectoring for narrow tilting vehicle.

Torque controller

SATV. To compensate the counter-steering behaviour, the easiest way is to set the vectoring torque proportional to the derivative of steer angle as follows

$$\Delta T_r = K\dot{\delta} \tag{30}$$

where K is the control gain to be adjusted for an expected controller performance. This control parameter is chosen to set the bandwidth of the TV controller in such a way that its speed of response is faster than that of the vehicle yaw moment and slower than that of the wheel motor torque. A simple iteration loop can be utilized to enhance this task (Figure 4).

When the rider is willing to turn, the vectoring torque is activated to make the vehicle yaw to the opposite direction and roll to the same direction as the rider wishes until reaching the steady state.

TCTV. After the virtual rider controls the vehicle yaw rate, the $\dot{\varphi}$ equals to the desired and $\ddot{\varphi}$ is assumed equal to zero. Then, from the yaw dynamics in equation (21), the steady-state steer angle can be presented as follows

$$\delta_{ss} = \frac{l}{v}\dot{\varphi} - \frac{2b_r}{C_\gamma l}\Delta T_r \tag{31}$$

Substitute equation (31) into the roll dynamic equation (21) to obtain a rewritten presentation as follows

$$\ddot{\theta} = \frac{1}{I_x}\left[\left(mgh - 2\lambda_\gamma h\right)\theta - C_d\dot{\theta} + 2C_\gamma h\beta - mh^2\dot{\theta}^2\theta - C_\gamma h\left(\frac{l}{v}\dot{\varphi} - \frac{2b_r}{C_\gamma l}\Delta T_r\right)\right] \tag{32}$$

By assuming $\dot{\theta}$ and $\ddot{\theta}$ are zero in steady state, one can obtain the following equation

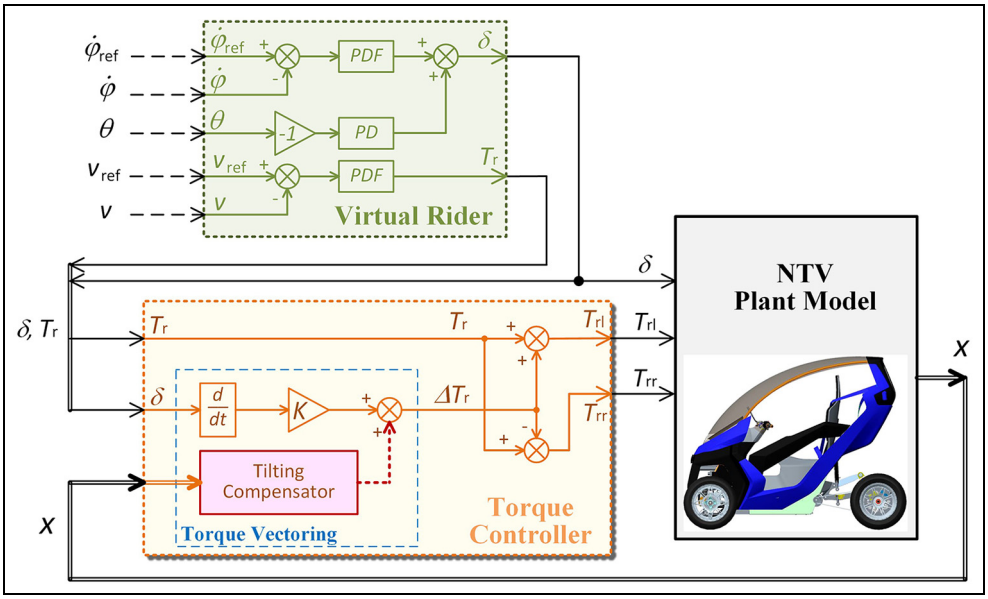

Figure 5. The control block diagram of torque vectoring.

$$\ddot{\theta} = \frac{h}{I_x}\left[(mg - 2\lambda_\gamma)\theta + 2C_\gamma\beta - \frac{C_\gamma l}{v}\dot{\varphi} + \frac{2b_r}{l}\Delta T_r\right] = \sigma \tag{33}$$

If the control signal is designed as

$$\sigma = \frac{h}{I_x}\frac{2b_r}{l}K\dot{\delta} = K'\dot{\delta} \tag{34}$$

the vectoring torque for roll stability improvement can be delivered from equation (33) as

$$\Delta T_r = K\dot{\delta} + \Psi \tag{35}$$

where

$$\Psi = \frac{l}{2b_r}\left[C_\gamma\delta - (mg - 2\lambda_\gamma)\theta - 2C_\gamma\beta\right] \tag{36}$$

Comparing equation (35) with equation (30), one can find that there is an additional component Ψ, which is defined as the tilting compensator (TC). The TCTV method can manage the vectoring torque to reduce the counter-steering during a turn. The block diagram of the TV-based drive assistance system is shown in Figure 5.

Torque management. As the main source of pure electric vehicles, the batteries perform significant roles in vehicle propulsion. Considering the limit output power of battery and electric motors, the torque controller should adjust the output torque to protect the equipment from over-current. The available torque can be represented as follows

$$T_{avi} = \min\left(T_{m,rated}, \frac{\min(P_{m,rated}, P_{b,avi})}{\omega_m}\right) \tag{37}$$

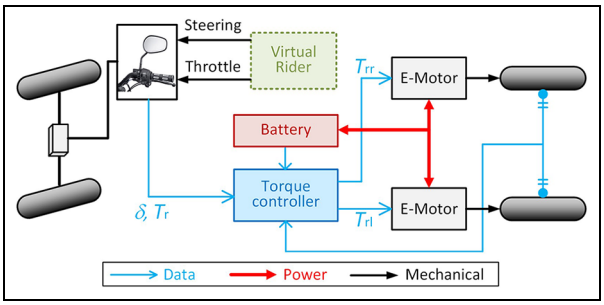

Figure 6. The diagram of torque vectoring for narrow tilting vehicle.

where $T_{m,rated}$ and $P_{m,rated}$ are the rated torque and power of wheel motor from manufacturer; $P_{b,avi}$ is the maximum output power from vehicle battery management system (BMS) based on the charging status of battery. Then, the torque output is managed considering the available torque as

$$T'_r = \min(T_r, T_{avi}) \tag{38}$$

$$\Delta T'_r = \min[\Delta T_r, (T_{avi} - T'_r)] \tag{39}$$

Then, the final torque applied on the left and right rear wheels can be represented as follows

$$\begin{cases} T_{rl} = T'_r + \Delta T'_r \\ T_{rr} = T'_r - \Delta T'_r \end{cases} \tag{40}$$

The torque drive system of NTV is shown in Figure 6, where the data flow, electric power flow, and mechanical drive are given with blue, red, and black arrows, respectively.

Control objectives and stability analysis. This article focuses on the suppression of the roll motion. For the NTV, the

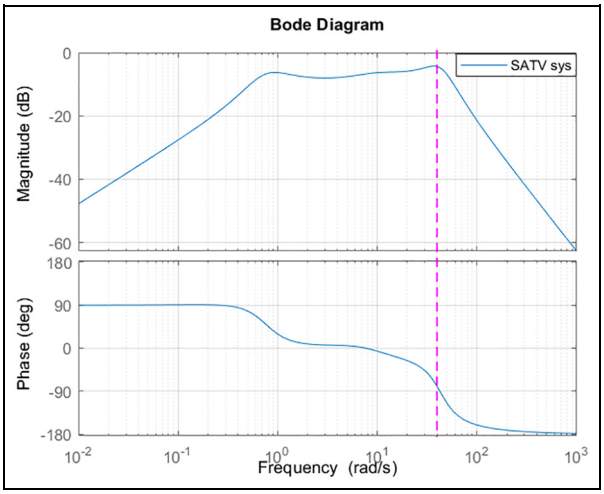

Figure 7. Bode diagram of SATV-based closed-loop system.

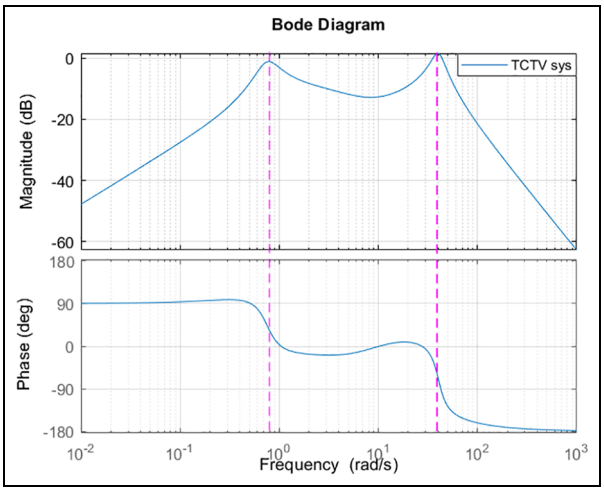

Figure 8. Bode diagram of TCTV-based closed-loop system.

roll motion is the most significant index as the lack of roll stability will make the NTV fall down easily when it turns in a corner. The yaw motion will not affect the stability of vehicle and it aims to track the desired route which is not the primary control objective. In addition, the virtual rider in the closed-loop system aims to track the yaw rate. This can easily adjust the performance of yaw rate and side-slip angle of vehicle by the operation of virtual rider and is not considered in the proposed torque controller. Thus, the control objective of the drive assistance system is to suppress the roll rate to zero in finite time in the presence of unpredictable operation (the steer angle δ) from the rider.

The Bode plots of closed-loop system are shown in Figures 7 and 8 for SATV- and TCTV-based systems, respectively. In the Bode diagram, when the magnitude (in dB) is below zero, the phase is greater than $-180°$ in all circumstances. It shows that the closed-loop system will not amplify the system error and has the ability to eliminate the error with damping applied on the closed-loop system. Comparing the Bode figures of SATV and TCTV, the TCTV-based closed-loop system has better

Table 1. System parameters of NTV.

Description	Symbol	Value	Unit
Total vehicle mass	m	200.0	kg
Height of vehicle COG	h	0.5	m
Gravitational constant	g	9.81	m/s^2
Distance from COG to front axle	l	0.7	m
Distance from COG to rear axle	lr	0.9	m
Length of track of rear axle	b_r	0.7	m
Vehicle roll moment inertia	I_x	18	$kg\,m^2$
Vehicle yaw moment inertia	I_z	80	$kg\,m^2$
Front/rear wheel radius	$R_{fl/rj}$	0.5	m
Front/rear wheel rotational inertia	$J_{fl/rj}$	0.2	$kg\,m^2$
Front cornering stiffness	C_f	3500	N/rad
Rear cornering stiffness	C_r	5480	N/rad
Front camber stiffness	λ_f	1000	N/rad
Rear camber stiffness	λ_r	2000	N/rad

COG: centre of gravity.

Table 2. Controller parameter settings.

Description	Symbol and value
Virtual rider	$k_{p1} = 0.3$; $k_{i1} = 0.2$ $k_{p2} = 1$; $k_{d2} = 5$ $k_{p3} = 1$; $k_{i3} = 0.4$
Torque controller	$K = 50$ $T_{m,rated} = 50\,N\,m$ $P_{m,rated} = 1500\,W$

damping within the range of frequency between 0.8 and 40 rad/s (approximately 0.1–6 Hz), which covers the basic response speed of the vehicle and the rider. In normal driving cases, the closed-loop system performs better using the TCTV torque controller. The NTV system with both TV approaches is proved to be stable from low to high frequency.

Simulation results

The NTV parameters used for the simulation are obtained from the work by Gohl[28] (Table 1). The simulation validations are carried out by tracking the route of a step yaw rate in two case studies. The first case is that the vehicle driven into a turn at a constant speed and the second case is that the vehicle accelerating during a turn. For a fire comparison among different torque controllers of SATV controller, TCTV controller, and the traditional controller without TV technology, all the tests use the same rider model and vehicle plant model. The parameter settings of the virtual rider model and torque controller are shown in Table 2.

Due to the requirements of counter-steering process, it is a challenge for new riders to balance the vehicle and follow the path simultaneously when driving an NTV. Two simulation cases are designed to verify the control performances. The first case is chosen as

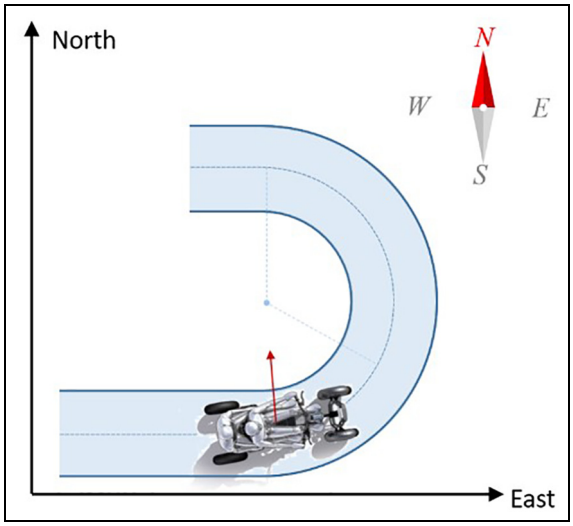

Figure 9. Path of vehicle with left turn in simulation.

driving into a turn to the left under a constant speed. With a step change on the steering reference, the torque controller will assist the rider to tilt the vehicle. The performance will validate the effectiveness of the designed controller on counter-steering reduction. The second case is chosen as accelerating during a left turn. Accelerating or decelerating in a turn has the risk to cause vehicle instability. Thus, this operating case is chosen to verify the stability improvements of the designed controller.

Left turn under constant speed

The case study is to simulate the dynamic response of an NTV to start a turn in simulation. The vehicle is driven forward under a constant speed of 5 m/s as an initial state. Then, the rider starts to turn the vehicle to track the path of a circle with the radius of 15 m, as shown in Figure 9. The desired command to the virtual rider is a step change of yaw rate to achieve a perfect path following. However, as the vehicle itself has its own yaw inertia, as well as roll inertia, it is not possible to reach the target yaw rate immediately. Thus, the step change of yaw rate reference actually acts as a sudden disturbance to the torque controller to verify its transient response. In conventional roll and yaw control method, the rider should counter-steer the front wheels to lean the vehicle into an opposite direction until the roll angle achieves the desired value to maintain its roll stability. Then, the rider steers the front wheels to yaw the vehicle into the target direction for path following. All these reactions have to be completed within seconds. With the assistance of TV, the counter-steering requirements from the rider will be reduced as the roll stability can be maintained via the torque controller through TV technology.

Figure 10 shows the dynamic response of the two inputs, the steering angle and vectoring torque, as well as the system states of vehicle side-slip angle, yaw rate, lateral acceleration, and roll rate. The comparisons are among the steering and torque control by the rider, the traditional TV approaches, and the SATV- and TCTV-based torque control to assist the same rider from the virtual model. In the steering angle comparison, both the SATV- and TCTV-based torque control methods have reduced the counter-steering requirements from the rider. The traditional TV approaches focused on the yaw moment of the vehicle to provide a steady-state torque when the vehicle is turning, while the proposed SATV and TCTV provide a transient torque when the vehicle starts to turn. In the vectoring torque comparison, the TCTV has less oscillation comparing with the SATV due to the compensation of tilting dynamics. In the system states, the vehicle velocity and roll angle of all the four controllers have no obvious difference. The steady-state target value of the yaw rate calculated from equation (25) is 19°/s. The yaw rate and lateral acceleration of the TCTV-based torque control have less oscillation comparing with the other three methods. The steady-state target value of the side-slip angle is 2.9°. The performance of side-slip angle is significantly caused by steering angle so it has the same response to that of the steering angle. The roll rate of the TCTV-based torque control has the best performance with less peak roll rate and less oscillation. The SATV-based torque control shows better performance than the steering and torque control by the rider but worse than that of the TCTV-based torque control.

The states' tracking error is shown in Figure 11 to get a clearer comparison. It can be seen from the results of tracking error performance that the proposed controllers provided better performance in transient response with less oscillation rate and less maximum tracking error. In addition, the error has been eliminated to zero within about 4 s from the disturbance occurs. Thus, the proposed controllers achieve not only the stability of roll dynamic but also that of the steady-state as well.

The quantitative comparison result of maximum state tracking error and integral absolute error (IAE) is summarised in Table 3. The proposed TV control algorithm has less maximum error and oscillation comparing with the conventional rider controlled torque response and traditional TV approach. With the usage of TCTV, the counter steering from virtual rider is eliminated and the maximum error of steering control is reduced about 74%. Other performances of the system dynamic response have also been improved because of the drive assistance by TV. The side-slip angle, yaw rate, lateral acceleration, and roll rate have 35%, 58%, 36%, and 28% less maximum tracking error of steady state, respectively. To make the comparison more obvious to readers, the indices of the maximum error and IAE in percentages of their steady-state value, Figure 14 shows the bar chart to compare the dynamic performance of the system states.

Speed acceleration during a turn

The constant speed turn of an NTV is much easier to balance the vehicle, while the speed change of both

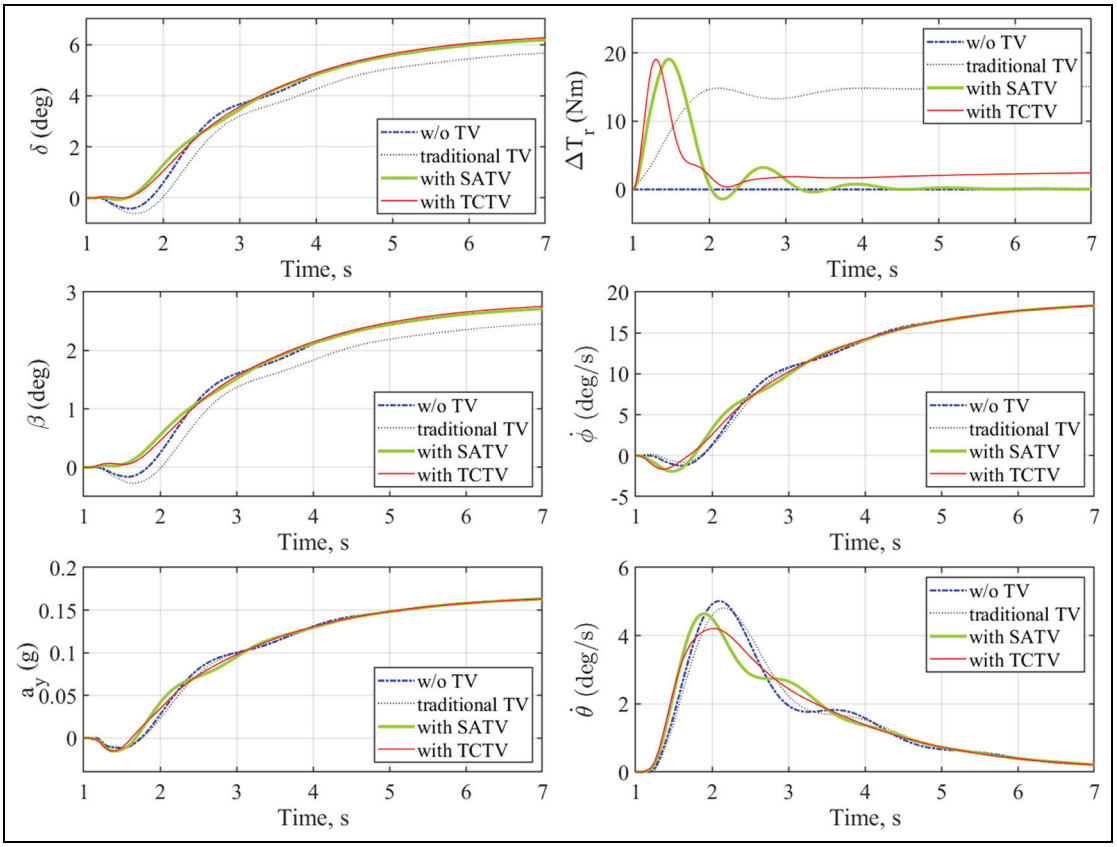

Figure 10. Simulation result of case 1 – left turn under constant speed.

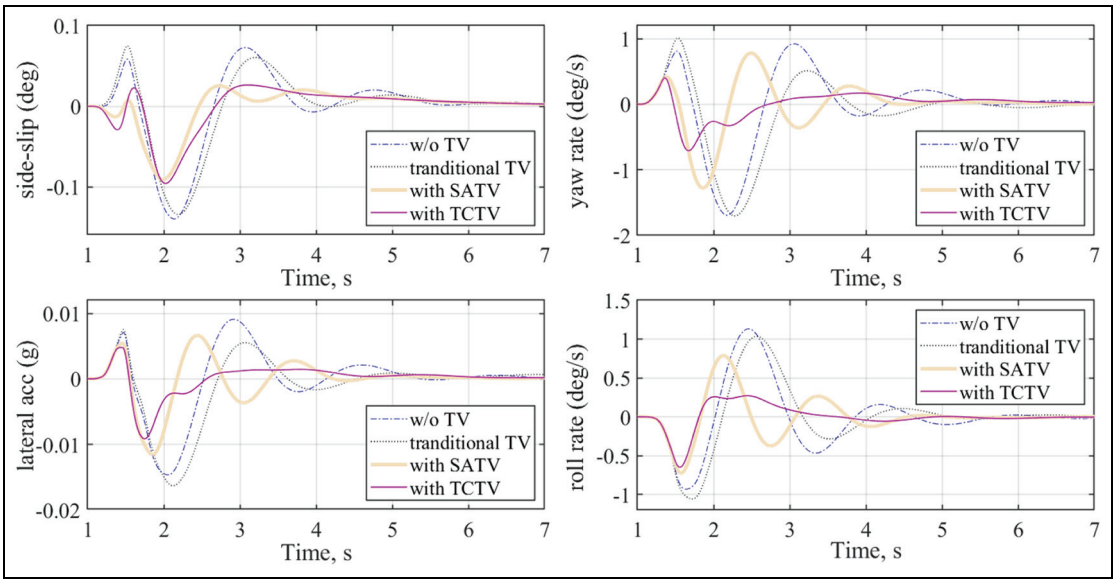

Figure 11. States' tracking error comparison of case 1.

acceleration and deceleration will cause more instability of the vehicle especially the roll dynamics. The second case is designed under the condition of accelerating the speed of NTV during a turn. The vehicle is driven at the speed of a constant 5 m/s in the initial state and yaw rate of about 5.8°/s in the steady state. Then, the rider increases the propulsion torque to accelerate the vehicle.

Figure 12 shows the dynamic response of an NTV in this case, including two inputs and four system states. The states' tracking error comparison is shown in Figure 13. Similar to the previous case, the SATV- and TCTV-based torque controls have reduced the counter-steering requirements from the rider when accelerating in a turn. In the yaw rate and roll rate comparison, the TCTV performs the best with the least peak error and

Table 3. Maximum state tracking error and integral absolute error comparison among different controllers of both cases.

Indices	Variables	Case 1: Drive into a turn with constant speed				Case 2: Speed acceleration during a turn			
		Without TV	Traditional TV	With SATV	With TCTV	Without TV	Traditional TV	With SATV	With TCTV
Maximum track error	Counter-steering angle (°)	0.553	0.311	0.107	0.006	0.053	0.013	0.0027	0
	Side-slip angle (°)	0.1442	0.138	0.0943	0.101	0.0184	0.0165	0.0173	0.0162
	Yaw rate (°/s)	1.763	1.82	1.307	0.719	0.0834	0.0539	0.0673	0.0447
	Lateral acceleration (×0.01g)	1.51	1.711	1.19	0.933	0.0687	0.0316	0.0332	0.0229
	Roll rate (°/s)	1.166	1.086	0.803	0.653	0.049	0.0261	0.0302	0.0169
Integral absolute error	Side-slip angle (°)	0.297	0.290	0.160	0.185	0.0266	0.0246	0.0242	0.0239
	Yaw rate (°/s)	3.66	3.43	2.07	1.24	0.137	0.0793	0.0733	0.0535
	Lateral acceleration (×0.01g)	3.136	3.217	1.861	1.199	0.118	0.0619	0.0572	0.0367
	Roll rate (°/s)	2.586	2.426	1.52	0.832	0.0628	0.0332	0.0263	0.0361

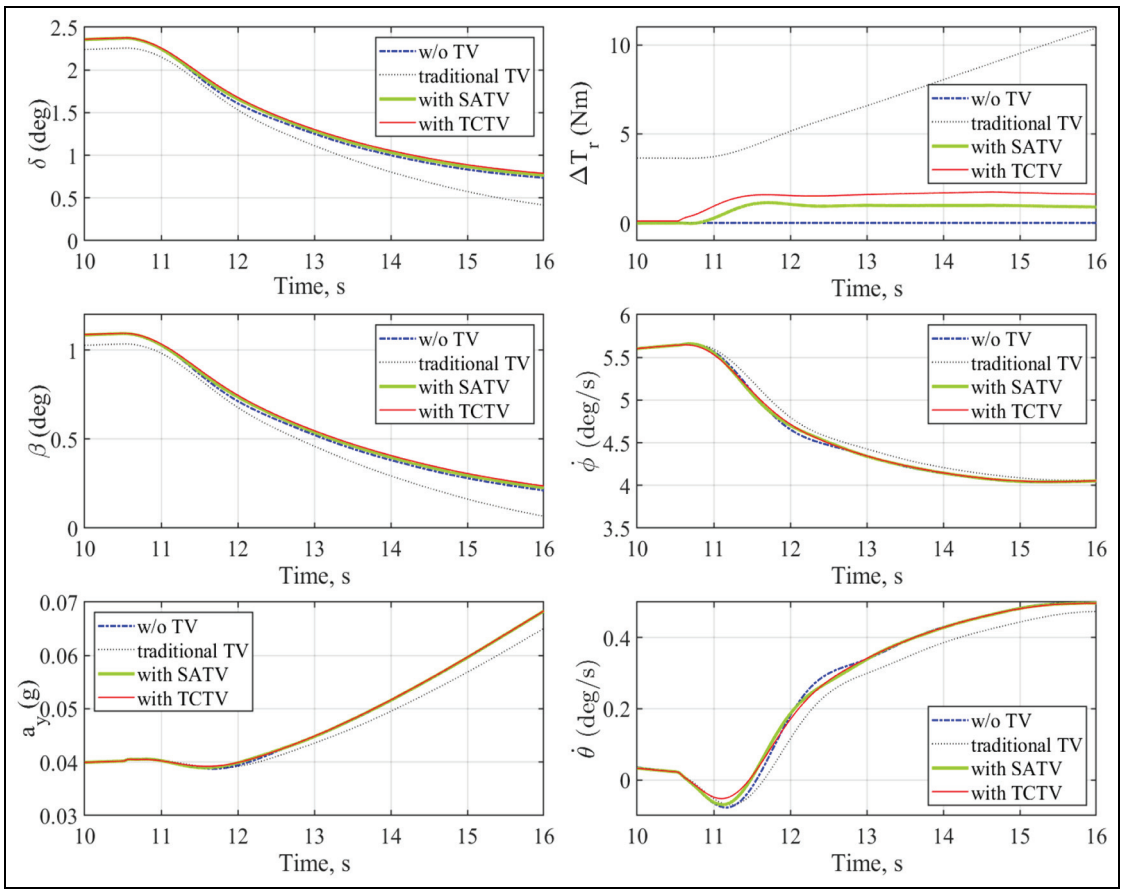

Figure 12. Simulation result of case 2 – acceleration during a turn.

faster rising time. To make it more obvious to readers, the numerical results and bar chart comparison of maximum tracking error and IAE to steady-state value are shown in Table 3 and Figure 14. The counter-steering requirements have been fully eliminated from the rider. The TCTV method has the ability to reduce the maximum error of steady-state value in steer angle, side-slip, yaw rate, lateral acceleration, and roll rate by 35%, 44%, 59%, 73%, and 55%, respectively.

The cases aim to verify the control performance under a sudden disturbance on references in Case 1 and a time-varying disturbance on references in Case 2. The different types of disturbances show that the two cases achieved different performances in maximum error,

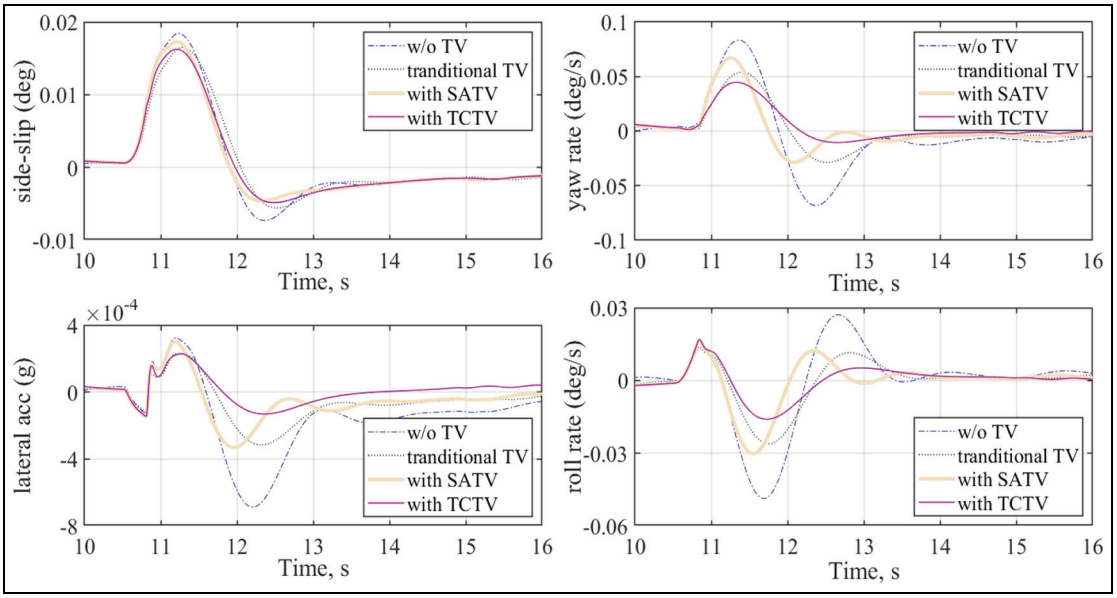

Figure 13. States' tracking error comparison of case 2.

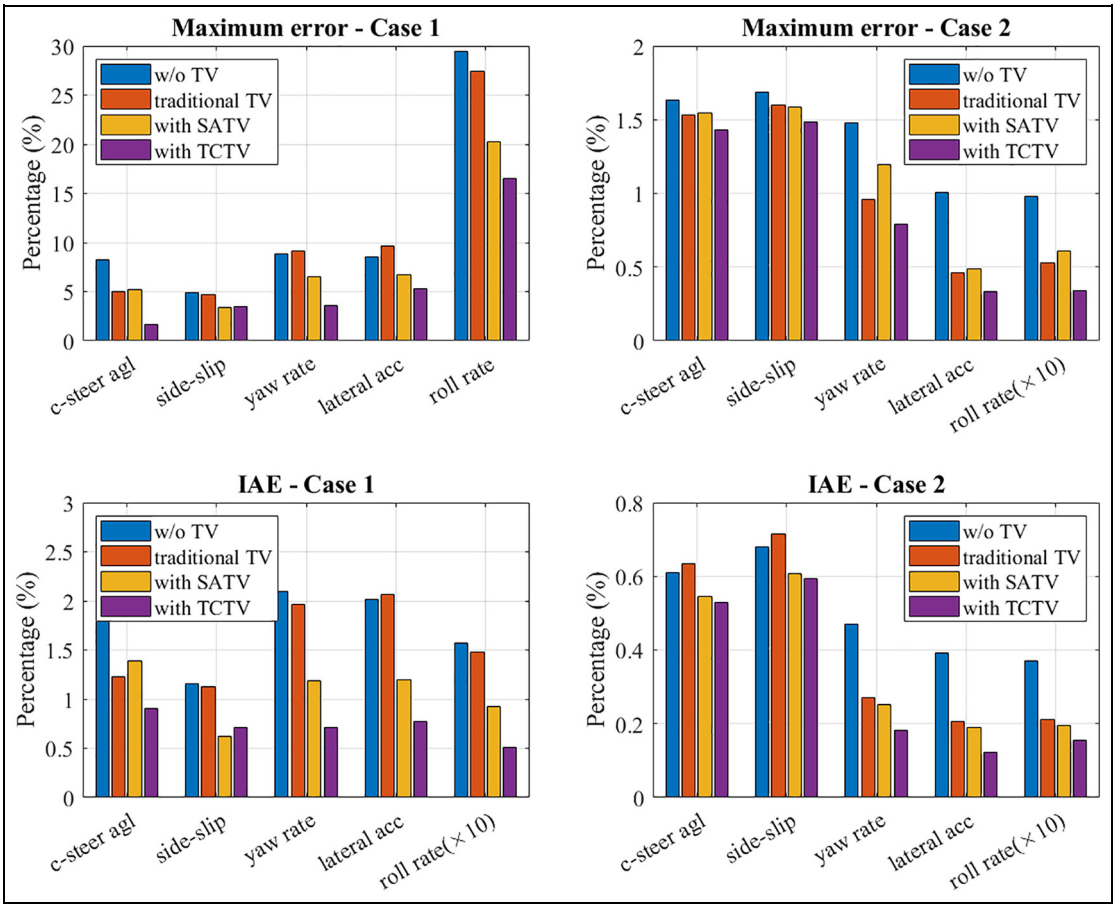

Figure 14. Comparison of performance indices among different torque controllers.

oscillation rate, and IAE value. From both the cases, it can be concluded that with the use of TV drive assistance method, the counter-steering requirements can be fully eliminated from the rider, the maximum tracking error and oscillation rate of counter-steering angle can be reduced more than one-third of that without using TV, and the control performance of yaw rate, lateral acceleration, and roll rate can be improved with a

quarter to half reduction in the peak tracking error. Comparing the TCTV and the SATV methods, the TC eliminates the bad performance of maximum error and oscillation rate in SATV with further improvement in roll stability of NTV. The improvement is more obvious in a turn with speed acceleration, which has more challenges in balancing the vehicle. As the same rider model has been used in all tests, the NTV equipped with the TV-based drive assistance system can help the rider, especially the new rider to balance the vehicle during a turn under both a constant speed and an increasing speed. Therefore, an NTV equipped with the drive assistance system will be easy to be ridden by any type of rider with improved roll stability.

Conclusion

This article has designed two TV-based drive assistance systems to help the rider in balancing the NTV during a turn and simplify the steering process. The two assistance systems, the SATV and the TCTV, have been validated in simulation with the same rider model. From the simulation results, both TV-based assistance methods eliminate the counter-steering requirements with improved roll stability in balancing the vehicle in the cases of constant speed turn and speed acceleration in a turn. In addition, with the TC, the unwanted maximum tracking error and oscillation rate of their steady-state value have been reduced in all the dynamics of system states. The TCTV-based drive assistance system can be used to help riders to balance the NTV in a turn without the dependency of riding experience from the riders.

Acknowledgements

The research presented in this article was undertaken as part of the Range of Electric SOlutions for L-category VEhicles (RESOLVE) project.

Declaration of conflicting interests

The author(s) declared no potential conflicts of interest with respect to the research, authorship, and/or publication of this article.

Funding

The author(s) disclosed receipt of the following financial support for the research, authorship, and/or publication of this article: This work is funded through the European Funding for Research and Innovation (Horizon 2020), grant number 653511.

ORCID iD

Yaxing Ren https://orcid.org/0000-0002-8716-6024

References

1. Ren Y, Dinh Q, Marco J, et al. Nonlinearity compensation based tilting controller for electric narrow tilting vehicles. In: *Proceedings of the 5th international conference on control, decision and information technologies (CoDIT)*, Thessaloniki, 10–13 April 2018, pp.1085–1090. New York: IEEE.
2. RESOLVE project, 2018, http://www.resolve-project.eu/events/
3. Frezza R and Beghi A. A virtual motorcycle driver for closed-loop simulation. *IEEE Contr Syst* 2006; 26(5): 62–77.
4. Claveau F, Chevrel P and Mourad L. Non-linear control of a narrow tilting vehicle. In: *International conference on systems, man and cybernetics (SMC)*, San Diego, CA, 5–8 October 2014, pp.2488–2494. New York: IEEE.
5. Pojani D and Stead D. Sustainable urban transport in the developing world: beyond megacities. *Sustainability* 2015; 7(6): 7784–7805.
6. Li L, Lu Y, Wang R, et al. A three-dimensional dynamics control framework of vehicle lateral stability and rollover prevention via active braking with MPC. *IEEE T Indus Electron* 2017; 64(4): 3389–3401.
7. Van Poelgeest A. *The dynamics and control of a three-wheeled tilting vehicle*. PhD Thesis, University of Bath, Bath, 2011.
8. Fajans J. Steering in bicycles and motorcycles. *Am J Phys* 2000; 68(7): 654–659.
9. Mourad L, Claveau F and Chevrel P. Direct and steering tilt robust control of narrow vehicles. *IEEE T Intell Transport Syst* 2014; 15(3): 1206–1215.
10. Snell A. An active roll-moment control strategy for narrow tilting commuter vehicles. *Veh Syst Dyn* 1998; 29(5): 277–307.
11. Van Den Brink CR and Kroonen HM. DVC – the banking technology driving the CARVER vehicle class. In: *7th international symposium on advanced vehicle control*, HAN University, Arnhem, Netherlands, 23–27 August 2004.
12. Kidane S, Alexander L, Rajamani R, et al. A fundamental investigation of tilt control systems for narrow commuter vehicles. *Veh Syst Dyn* 2008; 46(4): 295–322.
13. De Novellis L, Sorniotti A and Gruber P. Wheel torque distribution criteria for electric vehicles with torque-vectoring differentials. *IEEE T Veh Tech* 2014; 63(4): 1593–1602.
14. Sawase K and Sano Y. Application of active yaw control to vehicle dynamics by utilizing driving/breaking force. *JSAE Rev* 1999; 20(2): 289–295.
15. Koehler S, Viehl A, Bringmann O, et al. Energy-efficiency optimization of torque vectoring control for battery electric vehicles. *IEEE Intell Transport Syst Mag* 2017; 9(3): 59–74.
16. Sawase K, Ushiroda Y and Miura T. Left-right torque vectoring technology as the core of super all wheel control (S-AWC). *Mitsubishi Mot Tech Rev* 2006; 18: 16–23.
17. Sawase K and Ushiroda Y. Improvement of vehicle dynamics by right-and-left torque vectoring system in various drivetrains. *Mitsubishi Mot Tech Rev* 2008; 20: 14–20.
18. Kang J, Kyongsu Y and Heo H. Control allocation based optimal torque vectoring for 4WD electric vehicle. SAE Technical paper 2012-01-0246, 2012.

19. Yim S, Choi J and Yi K. Coordinated control of hybrid 4WD vehicles for enhanced maneuverability and lateral stability. *IEEE T Veh Technol* 2012; 61(4): 1946–1950.
20. Fallah S, Khajepour A, Fidan B, et al. Vehicle optimal torque vectoring using state-derivative feedback and linear matrix inequality. *IEEE T Veh Technol* 2013; 62(4): 1540–1552.
21. Her H, Koh Y, Joa E, et al. An integrated control of differential braking, front/rear traction, and active roll moment for limit handling performance. *IEEE T Veh Technol* 2016; 65(6): 4288–4300.
22. Kumar P, Merzouki R, Conrard B, et al. Multilevel modeling of the traffic dynamic. *IEEE T Intell Transport Syst* 2014; 15(3): 1066–1082.
23. Pacejka H. *Tire and vehicle dynamics*. New York: Elsevier, 2005.
24. Svendenius J. *Tire modeling and friction estimation*. PhD Thesis, Lund University, Lund, 2007.
25. Kidane S, Alexander L, Rajamani R, et al. Road bank angle considerations in modeling and tilt stability controller design for narrow commuter vehicles. In: *American control conference*, Minneapolis, MN, 14–16 June 2006, p.6. New York: IEEE.
26. Kidane S, Rajamani R, Alexander L, et al. Development and experimental evaluation of a tilt stability control system for narrow commuter vehicles. *IEEE T Contr Syst Technol* 2010; 18(6): 1266–1279.
27. Ohm DY. Analysis of PID and PDF compensators for motion control systems. In: *Proceedings of the industry applications society annual meeting*, Denver, CO, 2–6 October 1994, vol. 2, pp.1923–1929. New York: IEEE.
28. Gohl J, Rajamani R, Starr P, et al. Development of a novel tilt-controlled narrow commuter vehicle, 2006, http://www.its.umn.edu/Publications/ResearchReportsportdetail. html?id = 1057